GENES, CHROMOSOMES & CANCER 42:213–227 (2005)

RESEARCH ARTICLE

Efficacy of a Rapamycin Analog (CCI-779) and IFN-γ in Tuberous Sclerosis Mouse Models

Laifong Lee,[1] Paul Sudentas,[1] Brian Donohue,[1] Kirsten Asrican,[1] Aelaf Worku,[1] Victoria Walker,[1] Yanping Sun,[2] Karl Schmidt,[2] Mitchell S. Albert,[2] Nisreen El-Hashemite,[1] Alan S. Lader,[1] Hiroaki Onda,[1] Hongbing Zhang,[1] David J. Kwiatkowski,[1] and Sandra L. Dabora[1]*

[1]Division of Hematology, Brigham and Women's Hospital, Boston, MA
[2]Department of Radiology, Brigham and Women's Hospital, Boston, MA

Tuberous sclerosis complex (TSC) is a familial tumor disorder for which there is no effective medical therapy. Disease-causing mutations in the *TSC1* or *TSC2* gene lead to increased mammalian target of rapamycin (mTOR) kinase activity in the conserved mTOR signaling pathway, which regulates nutrient uptake, cell growth, and protein translation. The normal function of *TSC1* and *TSC2* gene products is to form a complex that reduces mTOR kinase activity. Thus, mTOR kinase inhibition may be a useful targeted therapeutic approach. Elevated interferon-gamma (IFN-γ) expression is associated with decreased severity of kidney tumors in TSC patients and mouse models; therefore, IFN-γ also has therapeutic potential. We studied cohorts of $Tsc2^{+/-}$ mice and a novel mouse model of *Tsc2*-null tumors in order to evaluate the efficacy of targeted therapy for TSC. We found that treatment with either an mTOR kinase inhibitor (CCI-779, a rapamycin analog) or with IFN-γ reduced the severity of TSC-related disease without significant toxicity. These results constitute definitive preclinical data that justify proceeding with clinical trials using these agents in selected patients with TSC and related disorders.

INTRODUCTION

Tuberous sclerosis complex (TSC) is an autosomal-dominant tumor disorder that can affect multiple organs, including the kidneys, brain, heart, and lungs (Gomez et al., 1999; Online Mendelian Inheritance in Man, 2003b). The incidence of TSC is 1:6,000, and an estimated 1–2 million individuals are affected worldwide (National Tuberous Sclerosis Association, 1994). Sporadic pulmonary lymphangioleiomyomatosis (LAM; Sullivan, 1998; Online Mendelian Inheritance in Man, 2003a) is a progressive pulmonary disorder that is genetically related to TSC because somatic mutations in *TSC1* or *TSC2* have been identified in abnormal lung tissue from LAM patients (Carsillo et al., 2000). Renal manifestations in TSC and LAM patients are significant because 60%–80% of TSC patients and 40%–50% of LAM patients develop kidney angiomyolipomas (tumors consisting of abnormal blood vessels, smooth-muscle cells, and fat cells; Sullivan, 1998; Gomez et al., 1999). TSC patients also can have a number of other medical problems, including epilepsy, cognitive impairment, behavioral problems, brain lesions (tubers and/or subependymal nodules), skin tumors (facial angiofibromas), cardiac tumors (rhabdomyomas), kidney cysts, renal cell cancer, and pulmonary abnormalities including LAM (Gomez et al., 1999; Dabora et al., 2001; Franz et al., 2001).

It is known that the *TSC1* and *TSC2* gene products, hamartin and tuberin, form a complex that inhibits mammalian target of rapamycin (mTOR) kinase activity in a conserved cellular signaling pathway (the mTOR pathway) that regulates nutrient uptake, cell growth, and protein translation (Consortium, 1993; van Slegtenhorst et al., 1997; Gao and Pan, 2001; Potter et al., 2001). A schematic diagram of the mTOR pathway is shown in Figure 1a. Key proteins in this pathway include PI3kinase, Akt, TSC1/TSC2, Rheb, mTOR, p70S6kinase (S6K), S6 ribosomal subunit (S6), and 4E-BP1. TSC2 is negatively regulated by Akt via phosphorylation (Manning et al., 2002; Potter et al., 2002). More recently, it has been shown that under low-energy conditions, TSC2 is activated by LKB1 (a serine/threonine kinase tumor suppressor that is mutated in Peutz–Jeghers syndrome) through AMP-dependent protein kinase (Inoki et al.,

Supported by: TS Alliance (to S.D. and L.L.); LAM Foundation (to N.E. and D.K.); NIH (NHLBI); Grant number: HL007680 (to T.S. and L.L.); NIH (NINDS); Grant number: NS31535 (to D.K.); NIH (NCI); Grant number: CA086248 (to S.D.); NIH (NIDDK); Grant number: DK066366 (to S.D.).

*Correspondence to: Sandra L. Dabora, Division of Hematology, Brigham and Women's Hospital, 75 Francis Street, CHNRB 6th Floor, Boston, MA 02115. E-mail: sdabora@partners.org

Received 16 April 2004; Accepted 2 September 2004

DOI 10.1002/gcc.20118

Published online 1 December 2004 in Wiley InterScience (www.interscience.wiley.com).

2003b; Corradetti et al., 2004). Inhibition of mTOR kinase occurs because tuberin is a GTPase-activating protein for Rheb, a small GTPase that regulates mTOR kinase activity (Garami et al., 2003; Inoki et al., 2003a; Saucedo et al., 2003; Stocker et al., 2003; Zhang et al., 2003b). When hamartin and tuberin are normal, the Rheb-GDP form is favored, and mTOR kinase activity is relatively low. When either hamartin or tuberin is defective, the Rheb-GTP form is favored, and mTOR kinase activity increases, resulting in hyperphosphorylation of the downstream targets S6K, S6, and 4E-BP1 (Fig. 1b). Rapamycin (also known as sirolimus) is an mTOR kinase inhibitor that is an approved drug (Rapamune®; Wyeth-Ayerst) for immunosuppression after organ transplantation. Because rapamycin has been shown to normalize dysregulated mTOR signaling in cells that lack normal hamartin or tuberin (Fig. 1c), mTOR kinase inhibition may be a useful approach to systemic therapy for TSC and/or LAM (Gao and Pan, 2001; Goncharova et al., 2002; Inoki et al., 2002; Kwiatkowski et al., 2002; Manning et al., 2002; Potter et al., 2002). In a cohort of TSC patients, we observed a decreased frequency of kidney angiomyolipomas in the presence of a high-expressing interferon-gamma (IFN-γ) allele (Dabora et al., 2002), so IFN-γ also may be a useful therapeutic agent for TSC and/or LAM. In addition, a dramatic reduction in the frequency of kidney tumors was reported in *Tsc2*$^{+/-}$ mice with elevated endogenous IFN-γ compared with *Tsc2*$^{+/-}$ mice with normal (low) levels of IFN-γ (Hino et al., 2002).

Although several important studies investigated the utility of rapamycin in rodent models of TSC, these investigations were limited to the evaluation of biochemical end points of unclear clinical significance in only a small number of animals after short-term treatment (Kenerson et al., 2002; El Hashemite et al., 2003a). These studies, along with in vitro data, provided justification for the recent initiation of the first single-institution trial of the use of rapamycin in TSC and LAM patients. Because the final results of this trial are not yet available and there is significant interest in implementing multicenter clinical trials for patients with TSC and LAM, we sought to accomplish definitive preclinical studies of rapamycin use, which would have the potential to influence and accelerate the initiation of such clinical trials. Here, we report the results of the effects of treatment with a rapamycin analog (CCI-779) or murine IFN-γ on cohorts of *Tsc2*$^{+/-}$ mice and on a novel mouse model of *Tsc2*-null tumors.

MATERIALS AND METHODS

Tsc2$^{+/-}$ Mice and MR Imaging

Tsc2$^{+/-}$ mice, which are heterozygous for deletion of exons 1–2, have been described previously (Onda et al., 1999). MR imaging was done using T2-weighted imaging with sectioning through the kidneys at 0.75-mm intervals. MR images were read by 3 blinded observers (S.D., Y.S., and K.S.) who independently determined the number of cystadenomas per kidney in each MR scan. The average of the 3 readings of each scan was used for the statistical analyses.

Quantitation of Kidney Cystadenomas in *Tsc2*$^{+/-}$ Mice by Necropsy and Histopathology

The number of kidney cystadenomas per kidney was determined at necropsy by examination of the surface of the kidneys under a dissecting microscope. For quantitative histopathologic analysis, each kidney was fixed and sliced at 1-mm intervals. The slices were then arranged sequentially for paraffin embedding, sectioning, and staining with hematoxylin and eosin (H&E). Slides were coded, and all cystadenomas were counted in a representative 6-μm section from each 1-mm kidney slice by an observer (L.L.) who was blinded to the treatment group. At the time of analysis, we observed that kidney sections were incomplete for 4 mice (of 68), which, therefore, were excluded from the quantitative histopathologic analysis. Cystadenomas that extended into more than one 1-mm slice were counted only once. Although kidney lesions easily can be divided into four subcategories (pure cysts, cystic lesions with papillary projections, cystic lesions filled with adenomatous growth, and solid adenomas), in this article, we use the term *cystadenomas* to mean this entire spectrum of kidney lesions as previously described (Onda et al., 1999).

Liver Hemangioma Grading in *Tsc2*$^{+/-}$ Mice

Liver hemangiomas were graded on a scale from 0 to 4, with 0 = no tumor; 1 = microscopic tumor only; 2 = tumor involving a single liver lobe; 3 = multiple lobes involved, with small tumors; and 4 = multiple lobes with large tumors. At necropsy, livers were examined and given a grade of 0 or 2–4. A single cross section of each liver lobe was stained with H&E and examined under the microscope to confirm the presence of liver hemangiomas in animals that had been graded 2–4. An animal graded 0 at necropsy was upgraded to 1 if at least one microscopic liver hemangioma was observed.

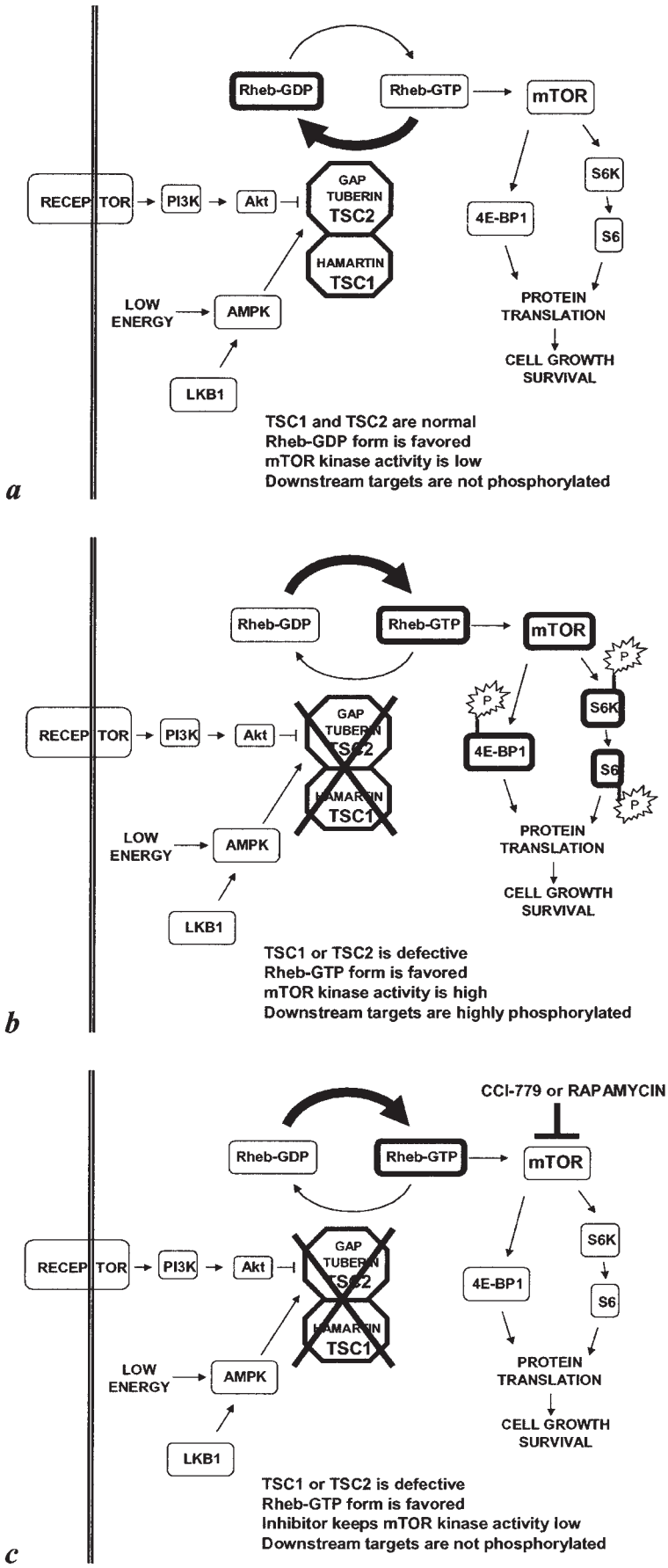

Figure 1. Schematic diagram of the mTOR signaling pathway.

Cell Lines, In Vitro Studies, and Genotyping

To isolate the NTC/T2null cell line, the subcutaneous tissue of a nude mouse was injected with a parent 110/T2null mouse embryo fibroblast (MEF) cell line derived from a $Tsc2^{-/-}$, $Trp53^{-/-}$ mouse embryo, and the tumor cells were recultured. The parent $Tsc2^{-/-}$, $Trp53^{-/-}$ MEF cell line, described previously, is known to have defective mTOR signaling (Zhang et al., 2003a). The $Trp53^{-/-}$ background is required because the $Tsc2^{-/-}$ genotype is embryonic lethal, and $Tsc2^{-/-}$ MEFs that are $Trp53^{+/+}$ tend to senesce and thus do not grow in culture. The NTC/T2null cell line rapidly and consistently produced TSC-related tumors in nude mice (7 of 8 untreated mice injected with 1.5 million cells developed measurable tumors between days 18 and 29, and 1 of 8 developed ascites and died on day 26). The control $Tsc2^{+/+}$, $Trp53^{-/-}$ MEFs (118/T2wt), described previously (Zhang et al., 2003a), also consistently produced tumors in nude mice (8 of 8 untreated mice injected with 2.4 million cells developed measurable tumor between days 11 and 13). All cells were grown in DMEM with 10% fetal calf serum in 5% CO_2, and serum deprivation was done for 48 hr. *Tsc2* genotyping was described previously (Onda et al., 1999). Rapamycin was obtained from Sigma-Aldrich, Inc. (St. Louis, MO); CCI-779 was obtained from Wyeth Pharmaceuticals (Madison, NJ); and murine IFN-γ was purchased from R&D Systems, Inc. (Minneapolis, MN).

Induction of Subcutaneous Tumors in Nude Mice

Nude mice (strain CD-1nuBR, 8-9 weeks old) were obtained from Charles River Laboratories, Inc. (Wilmington, MA). For the $Tsc2^{-/-}$ tumors, 16 nude mice were injected with 1.5 million NTC/T2null cells on day 0. For the control $Tsc2^{+/+}$ tumors, 16 nude mice were injected with 2.4 million 118/T2wt cells on day 0. This higher dose was used so that $Tsc2^{+/+}$ control tumors would form with a similar time course as that of the $Tsc2^{-/-}$ tumors. Cells were injected subcutaneously on the dorsal flank of 9- to 10-week-old nude mice, and tumors were measured with calipers 3 times a week. Tumor volume was calculated according to the formula $L \times W \times W \times 0.5$ (Torrance et al., 2001). All tumor-bearing animals were euthanized according to institutional animal care guidelines on the basis of tumor size or presence of an open ulcer. Nude mice bearing $Tsc2^{-/-}$ tumors were euthanized when tumor volumes were 4,000–10,000 mm^3 (days 32–49 for the untreated group); mice bearing $Tsc2^{+/+}$ tumors were euthanized at a lower tumor volume (2000–4000 mm^3; days 43–62) because open ulcers tended to develop in these mice. Tumor tissue was harvested for histopathologic analysis, and tumor lysates were prepared for immunoblot analysis.

Treatment of Mice with CCI-779 and IFN-γ

The $Tsc2^{+/-}$ mice were treated for 12 weeks (from 40 to 52 weeks old) with 4 mg/kg of CCI-779 administered by intraperitoneal (IP) injection 3 times per week. This dose and schedule were selected on the basis of pharmacokinetics and doses of rapamycin approved for immunosuppression after organ transplantation (Mahalati and Kahan, 2001) as well as consideration of the dosing of CCI-779 used in human clinical trials and rodent studies (Hidalgo and Rowinsky, 2000; Neshat et al., 2001; Podsypanina et al., 2001; Yu et al., 2001; Shi et al., 2002). We selected a short course of CCI-779 treatment (12 weeks) because there is some biochemical evidence of a response to short courses of rapamycin in TSC rodent models (Kenerson et al., 2002; El Hashemite et al., 2003). A 30 mg/ml stock solution of CCI-779 was made in ethanol (stored at 20°C for up to 1 week), diluted to 0.6 mg/ml in vehicle (0.25% PEG, 0.25% Tween-20), and used within 24 hr.

The $Tsc2^{+/-}$ mice were treated with murine IFN-γ for 44 weeks (from 8 to 52 weeks old) at a dose of 20,000 units (2.4 μg) IP 3 times per week. This dose was selected because it was well tolerated and had shown biological activity in a mouse model of chronic granulomatous disease (Jackson et al., 2001). We selected a longer duration for the IFN-γ treatment because data on both mice and humans suggested that IFN-γ may be useful for preventing the development of TSC-related kidney tumors (Dabora et al., 2002; Hino et al., 2002). Murine IFN-γ was diluted to 100,000 units/ml in PBS containing 0.1% mouse serum albumin (Sigma-Aldrich, Inc., St. Louis, MO), stored at 4°C, and administered within 24 hr.

All experiments were done according to animal protocols approved by our institutional animal protocol review committee and were compliant with federal, local, and institutional guidelines on the care of experimental animals. We did not observe significant toxicity from treatment with either CCI-779 or IFN-γ at the doses used in this study. All animals were checked 3 times per week, and their general behavior was monitored. $Tsc2^{+/-}$ mice were weighed weekly, and at the time of scheduled necropsy, there were no significant differences

(untreated average weight = 26.9 ± 3.1 g, CCI-779-treated average weight = 27.6 ± 4.0 g, IFN-γ-treated average weight = 27.2 ± 3.1 g). Our study sample comprised a total of 68 $Tsc2^{+/-}$ mice and 32 nude mice, and although 4 premature deaths occurred (3 of these mice were untreated), these did not cluster in either the CCI-779 or the IFN-γ treatment group and thus were not attributed to drug toxicity. In the $Tsc2^{+/-}$ three-arm trial, animals in all treatment groups appeared healthy until the scheduled necropsy when the animals were 52 weeks old, except for one animal in the untreated group that died prematurely.

In the nude mouse investigations, there were two untreated mice from the $Tsc2^{-/-}$ study that died early, including one animal that died on day 32 with a small (32 mm^3) tumor and another that showed clinical evidence of ascites several days prior to its death on day 26. These two animals were excluded from all analyses in order to avoid bias toward treatment with CCI-779 or IFN-γ. There was one $Tsc2^{+/+}$ tumor–bearing nude mouse in the CCI-779 group that died on day 54 with a small tumor (320 mm^3). Although this animal was included in the survival and tumor growth analyses, the results would not have changed significantly if it had been excluded. This death was not attributed to CCI-779 treatment because this was the only premature death in 36 mice treated with the same dose of CCI-779. There were no premature deaths in the IFN-γ-treated animals, but there was one IFN-γ-treated $Tsc2^{+/-}$ mouse that developed unilateral hydronephrosis.

Immunoblot Analyses, Immunohistochemistry for pS6, and Microscopy

Immunoblot analyses of tumor tissue and cultured cell lysates were performed as described previously (Kwiatkowski et al., 2002), and protein was detected by chemiluminescence (Pierce, Rockford, IL). For immunohistochemistry, kidney and tumor tissue was fixed, paraffin-embedded, and sectioned using standard methods, and unstained slides were pretreated with 20 μg/ml proteinase K. The primary antibody, anti-pS6-Ser235/236 (Cell Signaling Technology, Beverly, MA), was used at a 1:75 dilution. Immunoperoxidase staining was done using the Rabbit Immunocruz staining system, and nuclei were counterstained with Gill's formulation #2 hematoxylin. We obtained anti-Tsc2, HRP-conjugated secondary antibodies, and the Rabbit Immunocruz staining system from Santa Cruz Biotechnology (Santa Cruz, CA). Antiactin, proteinase K, and Gill's formulation #2 hematoxylin were obtained from Sigma-Aldrich, Inc. (St. Louis, MO). Anti-S6 antibody was synthesized by Sigma Genosys (The Woodlands, TX) by the immunization of rabbits with a synthetic peptide corresponding to the C-terminal 14-amino-acid residues of human S6.

Immunohistochemistry for pS6 expression in the kidney cystadenomas of the $Tsc2^{+/-}$ mice was scored by a blinded observer (L.L.) as strongly positive, weakly positive, or negative. All positives were grouped together for statistical analyses. In tumors that were induced in nude mice, pS6 expression was scored in nonnecrotic areas by two blinded observers (S.D. and L.L.) and graded on a scale from 0 to 3 (0 = no staining and 3 = strong staining). The average score from the two blinded observers was used for statistical analyses. Microscopy was done with a Nikon Eclipse TE 2000-E microscope using a 10× objective equipped with an Insight SPOT color camera (Micro Video Instruments, Inc., Avon, MA).

Statistical Analysis

Statview software (version 5.0) was used for all statistical analyses, and $P < 0.05$ was considered to indicate significance. The Fisher test was used for categorical variables, the t test was used for quantitative variables, and Mantel–Cox log-rank analysis for survival data. Following institutional guidelines for the care of experimental animals, all tumor-bearing mice with large or ulcerated tumors were euthanized; thus, the time of death for survival analysis was equivalent to the time of euthanasia because of severity of the tumor.

RESULTS

Treatment with CCI-779 or IFN-γ Decreased Severity of Kidney Cystadenomas in $Tsc2^{+/-}$ Mice

To evaluate the utility of CCI-779 or IFN-γ for treating TSC renal disease, we used $Tsc2^{+/-}$ mice for a three-arm preclinical study with an untreated control arm, a CCI-779 treatment arm, and an IFN-γ treatment arm. We used conventional $Tsc2^{+/-}$ mice (Onda et al., 1999) because they develop renal cystadenomas at high frequency by age 12 months and are a good model for the kidney angiomyolipomas that frequently develop in TSC and LAM patients. Because the $Tsc2^{+/-}$ colony is a mixed strain (129/SvJae-C57/BL6), sex-matched littermates were used as controls to avoid bias resulting from strain variation. Severity of kidney disease was assessed by three methods for quanti-

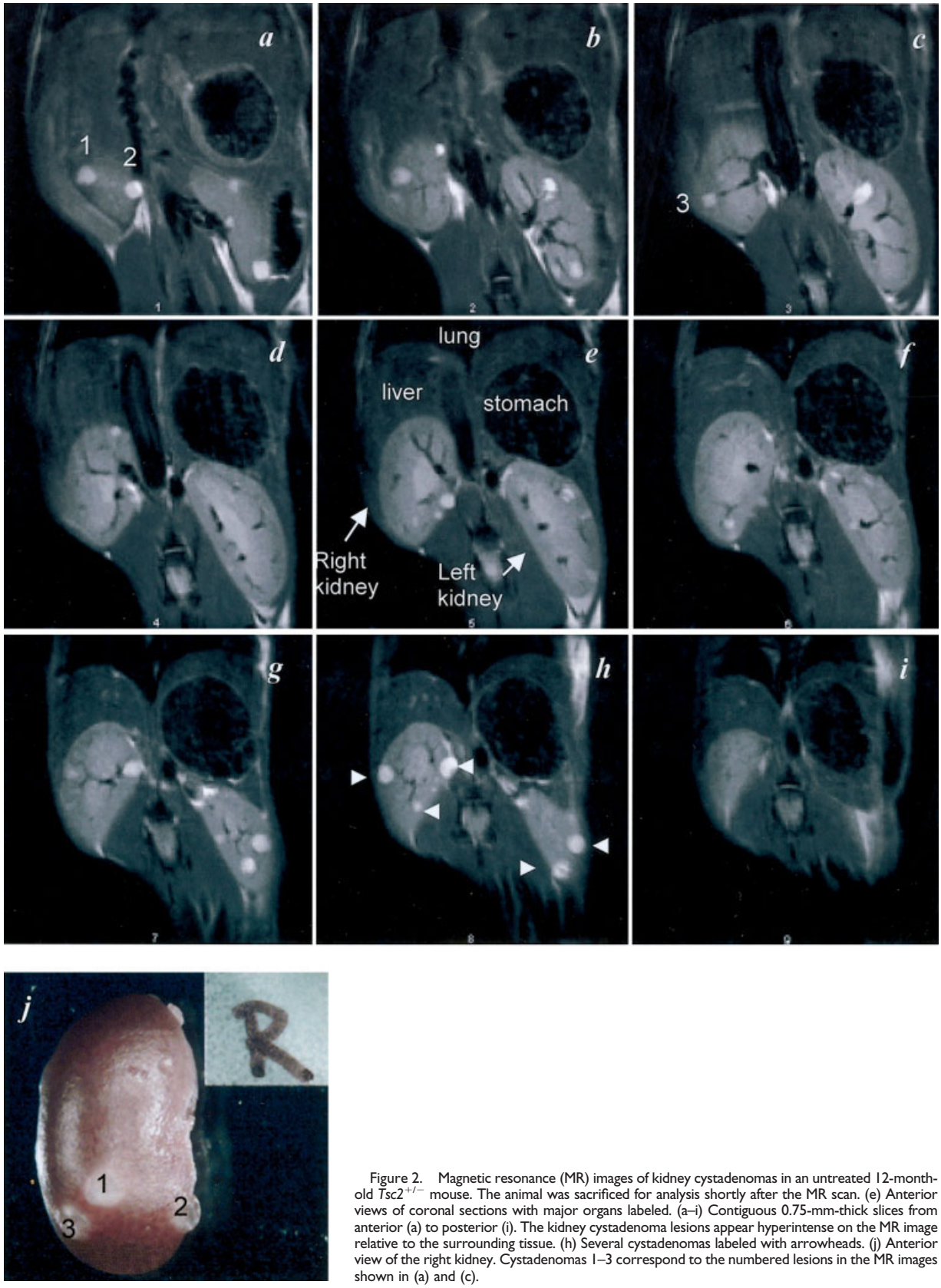

Figure 2. Magnetic resonance (MR) images of kidney cystadenomas in an untreated 12-month-old *Tsc2*$^{+/-}$ mouse. The animal was sacrificed for analysis shortly after the MR scan. (e) Anterior views of coronal sections with major organs labeled. (a–i) Contiguous 0.75-mm-thick slices from anterior (a) to posterior (i). The kidney cystadenoma lesions appear hyperintense on the MR image relative to the surrounding tissue. (h) Several cystadenomas labeled with arrowheads. (j) Anterior view of the right kidney. Cystadenomas 1–3 correspond to the numbered lesions in the MR images shown in (a) and (c).

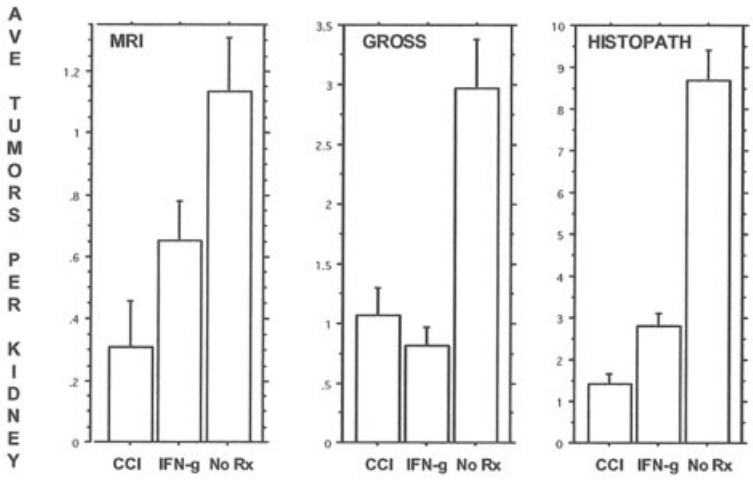

a

Group	*n* (mice)	MRI*: Ave. Cystadenomas per Kidney (Ave. ± Std. Err)	*P* value (MRI) (vs. untreated)
CCI-779	6	0.31 ± 0.15	0.003
IFN-γ	13	0.65 ± 0.13	0.027
Untreated	11	1.14 ± 0.17	
Group	***n* (mice)**	**GROSS: Ave. Cystadenomas per Kidney (Ave. ± Std. Err)**	***P* value (GROSS) (vs. untreated)**
CCI-779	21	1.07 ± 0.23	0.0001
IFN-γ	25	0.82 ± 0.16	<0.0001
Untreated	22	2.98 ± 0.41	
Group	***n* (mice)**	**HISTOPATH: Ave. Cystadenomas per Kidney (Ave. ± Std. Err)**	***P* value (HIST) (vs. untreated)**
CCI-779	21	1.43 ± 0.23	<0.0001
IFN-γ	23	2.80 ± 0.30	<0.0001
Untreated	20	8.70 ± 0.73	
Group	***n* (mice)**	**Ave. Grade Liver Hemangioma (Ave. ± Std. Err)**	***P* value (LIVER) (vs. untreated)**
CCI-779	21	0.29 ± 0.64	0.031
IFN-γ	25	0.36 ± 0.57	0.032
Untreated	22	1.05 ± 1.05	

*MR imaging not done on all animals

b

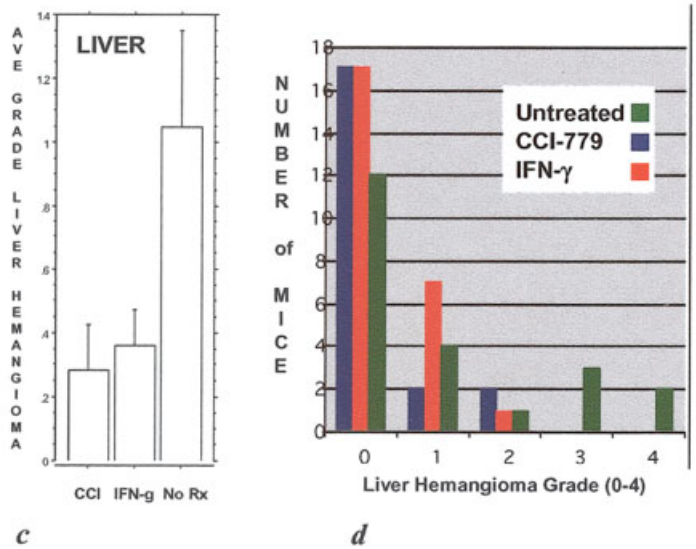

c *d*

Figure 3. Treatment of *Tsc2*$^{+/-}$ mice with CCI-779 or IFN-γ reduced severity of kidney cystadenomas and liver hemangiomas. The group treated with CCI-779 received 4 mg/kg by IP injection 3 times per week for 12 weeks (from 40 to 52 weeks old). The group treated with murine IFN-γ received 20,000 units IP 3 times per week for 44 weeks (from 8 to 52 weeks old). Severity of kidney disease was quantitated using three methods: magnetic resonance imaging (MRI), necropsy observation (GROSS), and quantitative histopathologic analysis (HISTOPATH). Data from the treatment groups are shown in (a) bar graph and (b) table format. (c) Average grade of liver hemangioma was reduced with CCI-779 or IFN-γ treatment. (d) Histogram of liver hemangioma grades showing reduced frequency of grade 0 tumors in the untreated cohort and the absence of higher-grade tumors (grades 3 and 4) in the CCI-779 and IFN-γ groups.

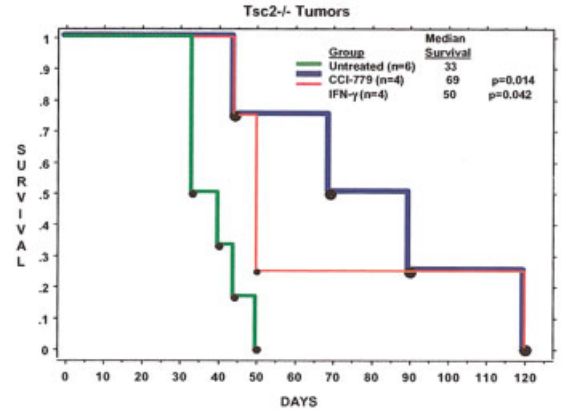

a

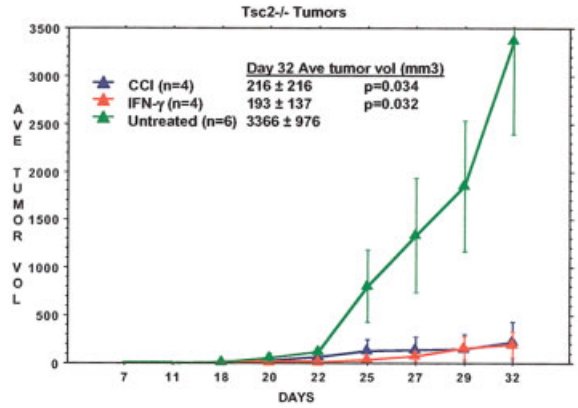

b

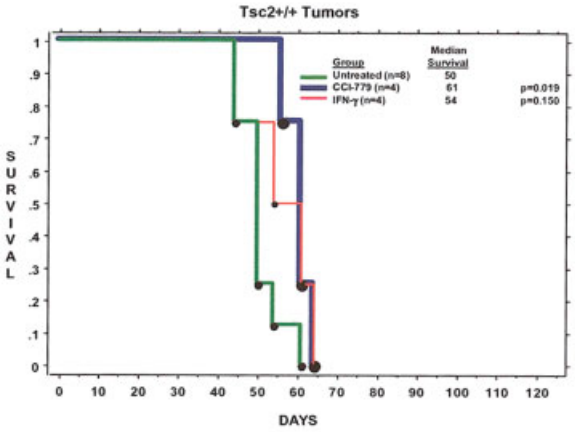

c

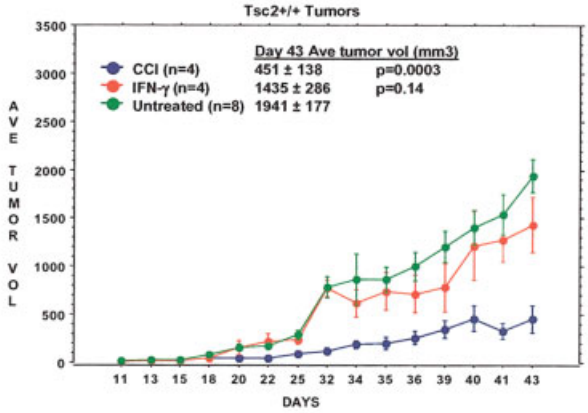

d

	Tsc2-/-			Tsc2+/+		
	No Rx	CCI-779	IFN-γ	No Rx	CCI-779	IFN-γ
Survival Range	32-50	43-120	43-120	43-61	55-65	43-65
Median Survival (days)	33	69	50	50	61	54
Increase in survival		109%	51%		22%	8%
P value (vs untreated)		0.014	0.042		0.019	0.15
Volume at day 32 or 43*	3366 ± 976	216 ± 216	193 ± 137	1941 ± 177	451 ± 138	1435 ± 286
Fold decrease (vs untreated)		16	16		4.3	1.3
P value		0.034	0.032		0.0003	0.14

*Day 32 for Tsc2-/-, Day 43 for Tsc2+/+

e

Figure 4.

tating the number of cystadenomas per kidney: (1) magnetic resonance (MR) imaging (Fig. 2 a–i), (2) gross kidney tumor counts (Fig. 2j), and (3) quantitative histopathology. Severity of disease was determined in all animals when they were 52 weeks of age because of the age-dependent development of kidney cystadenomas. To validate the utility of MR imaging for quantitating severity of disease, all MR images were obtained within 2 weeks of necropsy and histopathologic analysis. We observed a significantly higher burden of kidney cystadenomas per kidney in the untreated control group than in either the CCI-779 treatment group or the IFN-γ treatment group (Fig. 3a, b).

Treatment with CCI-779 or IFN-γ Decreased Severity of Liver Hemangiomas in *Tsc2*$^{+/-}$ Mice

Liver hemangiomas also develop in *Tsc2*$^{+/-}$ mice (Onda et al., 1999), although at a lower frequency than kidney cystadenomas. These liver tumors have histologic similarities to the smooth-muscle proliferation that occurs in the lungs of LAM patients (Kwiatkowski et al., 2002) and thus may be a useful animal model for LAM. We compared the severity of liver hemangiomas in the untreated *Tsc2*$^{+/-}$ cohort versus the two treatment groups (CCI-779 and IFN-γ). Liver tumors were graded on a scale from 0 to 4, and, consistent with the kidney results, we observed a higher burden of liver hemangiomas in the untreated control group than in either treatment group (Fig. 3c, d).

Treatment of Nude Mice Bearing *Tsc2*$^{-/-}$ Tumors with CCI-779 or IFN-γ Reduced Tumor Growth and Improved Survival

Although the conventional *Tsc2*$^{+/-}$ mouse is a good model for TSC renal disease and a useful model for pulmonary LAM, a disadvantage is that kidney and liver pathology are age-dependent, so using this model for preclinical studies is a slow process. We therefore developed a nude mouse model for TSC-related tumors by isolating a *Tsc2*$^{-/-}$, *Trp53*$^{-/-}$ MEF cell line (NTC/T2null) that forms tumors rapidly (within 3–4 weeks) and consistently in nude mice. Tumors that develop from the NTC/T2null cells are a good model for TSC-related tumors because TSC is a tumor-suppressor gene disorder, and LOH occurred in many of the tumors from TSC patients that have been analyzed previously (Henske et al., 1996; Henske et al., 1997; Niida et al., 2001).

We investigated the effects of treating nude mice bearing *Tsc2*$^{-/-}$ tumors with CCI-779 or IFN-γ as single agents (Fig. 4). A cohort of 16 nude mice was injected with NTC/T2null cells on day 0 and observed without intervention until day 18, when 4 mice started treatment with CCI-779, 4 mice started treatment with murine IFN-γ, and the remaining 8 mice were observed without treatment intervention. In the untreated group, all mice developed measurable tumors between days 18 and 29, and euthanasia of the animals was required between days 32 and 49 because the tumors were large. Mice in the CCI-779 and IFN-γ treatment groups also developed measurable tumors, but there was significantly improved survival and reduced tumor growth compared with that in the untreated controls (Fig. 4a, b). To evaluate whether the observed treatment effects were specific for *Tsc2*$^{-/-}$-derived tumors, we did a similar control experiment using a *Tsc2*$^{+/+}$, *Trp53*$^{-/-}$ MEF cell line (118/T2wt) and found a slight improvement in survival and a small reduction in the

Figure 4. Improved survival and decreased tumor growth from treatment with CCI-779 and IFN-γ in model of nude mice with *Tsc2*$^{-/-}$ tumors. (a–b) Cohort of 16 nude mice was injected with 1.5 million NTC/T2null cells on day 0 and observed without intervention until day 18, when treatment of 4 mice with CCI-779 (4 mg/kg IP 3 times per week), color-coded blue, and 4 mice with murine IFN-γ (20,000 units IP 3 times per week), color-coded red, was begun; the remaining mice continued to be untreated (color-coded green). Tumors were measured 3 times per week, and mice were euthanized if their tumors became large (4,000–10,000 mm^3) or they developed open ulcers. (a) Kaplan–Meier survival curves of the treatment groups. Mantel–Cox log-rank analysis showed a significant improvement in survival of both the CCI-779 ($P = 0.014$) and IFN-γ ($P = 0.042$) groups compared with the untreated (control) group. (b) Plot of average tumor volume versus day (to day 32) for the treatment groups. The average tumor volume in the untreated group was 16-fold greater than in both the CCI-779 (3,366 ± 976 mm^3 vs. 216 ± 216 mm^3, $P = 0.034$) and the IFN-γ (193 ± 137 mm^3, $P = 0.032$) groups on day 32, when it was necessary to euthanize 3 untreated animals because their tumors were large. (c–d) For the control experiments, *Tsc2*$^{+/+}$ tumors were generated by injection of a cohort of 16 nude mice with 2.4 million 118/T2wt cells on day 0. This slightly higher cell dose enabled the *Tsc2*$^{+/+}$ tumors to develop at a rate similar to that of the *Tsc2*$^{-/-}$ tumors. Animals were observed without intervention until day 18, when treatment of 4 mice with CCI-779 (4 mg/kg IP 3 times per week) and 4 mice with murine IFN-γ (20,000 units IP 3 times per week) was begun, with the remaining 8 mice remaining untreated, and mice were euthanized if their tumors became large (4,000–10,000 mm^3) or they developed open ulcers. (c) Kaplan–Meier survival curves of the treatment groups. Mantel–Cox log-rank analysis showed a significant difference between the CCI-779-treated and the untreated (control) groups ($P = 0.019$), but not between the IFN-γ-treated and the untreated groups ($P = 0.15$). (d) Plot of average tumor volume versus day (up to day 43) for the indicated treatment groups. The average tumor volume in the untreated group was 4.3-fold higher than that in the CCI-779 group (1,942 ± 500 mm^3 vs. 451 ± 276 mm^3, $P = 0.0003$) and only slightly (1.3-fold) higher than in the IFN-γ group (1,435 ± 574 mm^3, $P = 0.14$). (e) All the data described in this figure in table format (*average volumes determined until day 32 in the *Tsc2*$^{-/-}$ cohort and until day 43 in the *Tsc2*$^{+/+}$ cohort).

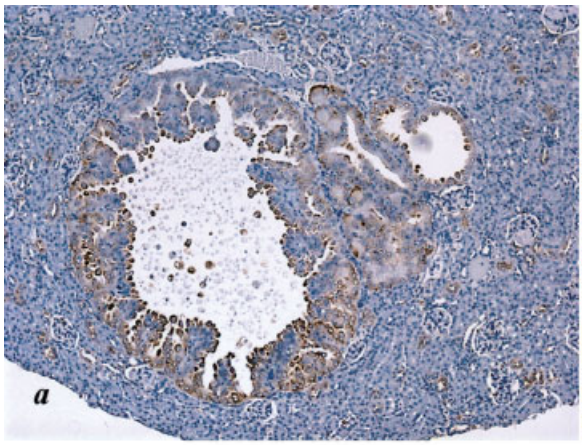

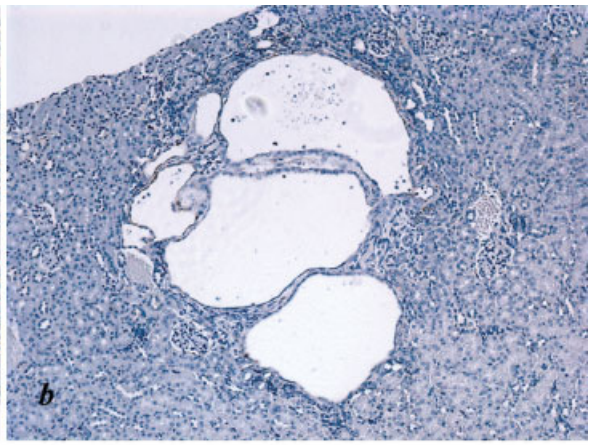

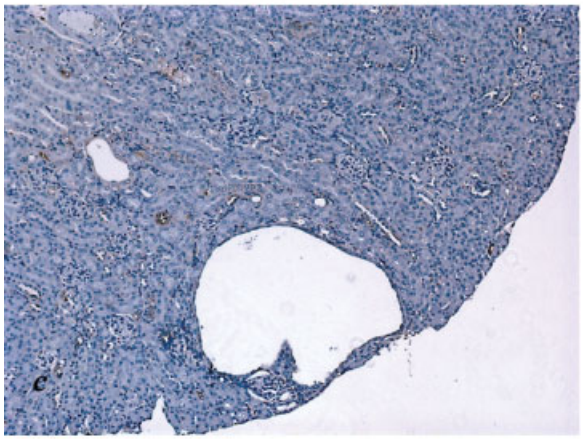

pS6 Expression in Kidney Cystadenomas

Group	No Rx	IFN-γ	CCI-779
N (mice)	7	10	10
Total Cystadenomas	99	53	17
PS6 positivie cystadenomas	87	35	5
% pS6 positive	88%	66%	29%
P value (vs. untreated)		0.002	<0.0001

d

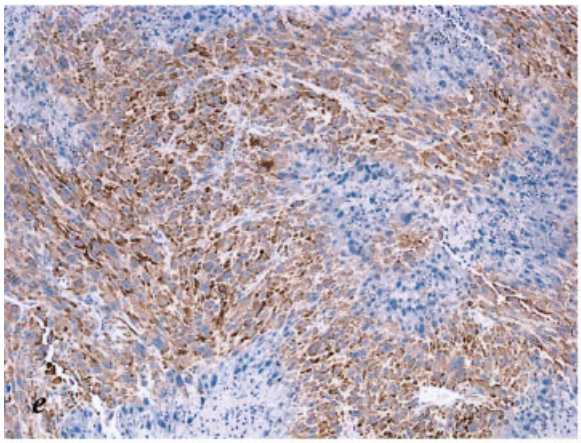

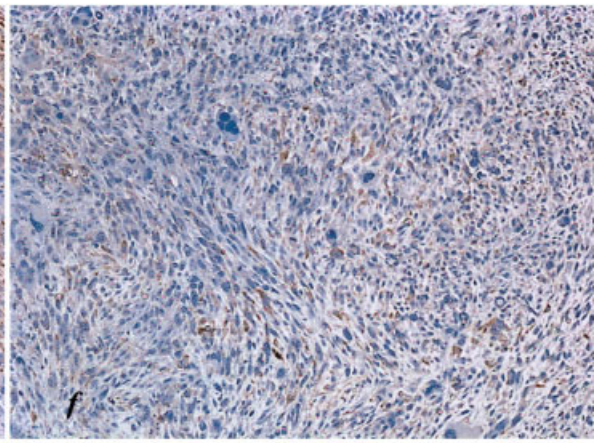

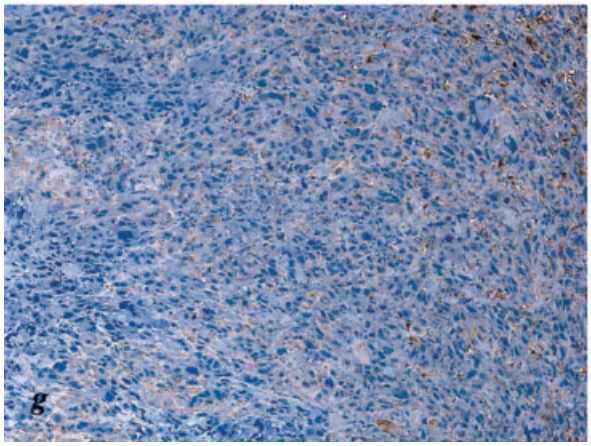

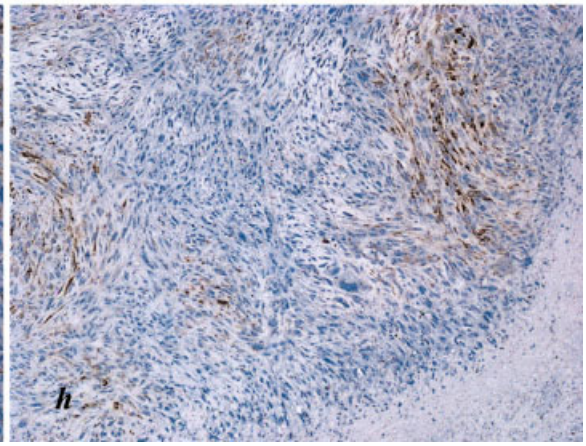

Figure 5.

tumor growth only in the CCI-779 group, not in the IFN-γ group (Fig. 4c, d).

Both CCI-779 and IFN-γ showed measurable antitumor activity in our nude-mouse model of $Tsc2^{-/-}$ tumors, but with some differences between the two treatment groups. In nude mice bearing $Tsc2^{-/-}$ tumors, median survival increased by 109% with CCI-779 treatment (33 days untreated vs. 69 days CCI-779-treated), and there was a 16-fold reduction in tumor growth. Although CCI-779 also improved survival and decreased tumor growth in the $Tsc2^{+/+}$ tumors, this change was much less dramatic because median survival increased by only 22% (50 days untreated vs. 61 days CCI-779-treated) and tumor growth showed only a 4.3-fold reduction. These results confirm that CCI-779 has general antitumor effects (Hidalgo and Rowinsky, 2000; Neshat et al., 2001; Podsypanina et al., 2001; Yu et al., 2001; Shi et al., 2002) and demonstrate the enhanced sensitivity of $Tsc2^{-/-}$ tumors to CCI-779.

The antitumor effects on $Tsc2^{-/-}$ tumors of IFN-γ treatment appear to be more specific than those of CCI-779. Treatment with IFN-γ significantly increased survival and decreased tumor growth in nude mice bearing $Tsc2^{-/-}$ tumors but not in $Tsc2^{+/+}$ tumors (Fig. 4e). Median survival increased by 51% with IFN-γ treatment (33 days untreated vs. 50 days IFN-γ-treated), and tumor growth showed a 16-fold reduction. Although improved survival was less striking in the IFN-γ-treated group than in the CCI-779-treated group, the effect of these two agents on tumor growth was similar.

Effects of Treatment on mTOR Signaling in Kidney Cystadenomas and $Tsc2^{-/-}$ Tumors

We evaluated mTOR signaling in kidney cystadenomas from untreated, CCI-779-treated, and IFN-γ-treated $Tsc2^{+/-}$ mice by using immunohistochemistry. We examined phosphorylated S6 (pS6) levels because elevated pS6 is a useful marker for the increased mTOR kinase activity that occurs in cells and tissues with defective hamartin or tuberin (Fig. 1b). We observed prominent pS6 staining in nearly all kidney cystadenomas from untreated $Tsc2^{+/-}$ mice (Fig. 5a). In contrast, pS6 staining was reduced in many cystadenomas from $Tsc2^{+/-}$ mice treated with CCI-779 (Fig. 5b) or with IFN-γ (Fig. 5c). We quantitated these results (Fig. 5d) and found a lower frequency of pS6-positive kidney cystadenomas in both the CCI-779 (29%, $P < 0.0001$) and the IFN-γ (66%, $P = 0.002$) group compared with the untreated control group (88%).

We used both immunoblot analysis and immunohistochemistry to investigate mTOR signaling in tumors from the TSC nude mouse model (Figs. 5e–h and 6). We first verified that the NTC/T2null cell line used to induce $Tsc2^{-/-}$ tumors in nude mice has aberrant mTOR signaling, as demonstrated by the high level of pS6 (Fig. 6a, lane 2) compared with that in the control $Tsc2^{+/+}$ cell line (Fig. 6a, lane 1). We also observed that a similar dose-dependent reduction in pS6 occurs when NTC/T2null cells in culture are treated with rapamycin or CCI-779 (for 4 hr), demonstrating the biological equivalence of these agents (Fig. 6a, lanes 3–8). In contrast, treatment of cultured NTC/T2null cells with IFN-γ did not reduce pS6 levels (Fig. 6a, lanes 9–10). Both immunohistochemistry and immunoblot analysis of tumor samples from untreated nude mice showed high pS6 levels in tumors derived from $Tsc2^{-/-}$ cells [Figs. 5e and 6b (lane 4)] and low pS6 levels in tumors derived from $Tsc2^{+/+}$ cells [Figs. 5h and 6b (lane 3)].

Treatment of nude mice bearing $Tsc2^{-/-}$ tumors with CCI-779 dramatically reduced pS6 levels in the tumors [Figs. 5f and 6b (lane 5)]. Although treatment with IFN-γ also reduced pS6 levels in $Tsc2^{-/-}$ tumors, the reduction was modest and not statistically significant [Figs. 5g, 6b (lane 6), and 6c]. We quantified pS6 immunohistochemistry (Fig. 6c, bottom) by scoring each tumor on a scale from 0 to 3, with 3 being the most intense staining. We quantified the immunoblot results by testing 2–3 lysates from every tumor sample in each group (Fig. 6c, top). The dramatic reduction in pS6 levels with CCI-779 treatment is consistent with a direct effect on the mTOR signaling pathway.

Figure 5. Immunohistochemical analysis of mTOR signaling in tumors from TSC mouse models. The brown stain (immunoperoxidase) indicates pS6 positive, the blue stain (hematoxylin counterstain) pS6 negative. (a) Kidney cystadenoma staining ps6 positive from an untreated $Tsc2^{+/-}$ mouse. (b) Reduced pS6 staining of a kidney cystadenoma from a CCI-779-treated $Tsc2^{+/-}$ mouse. (c) Reduced pS6 staining in a kidney cystadenoma from an IFN-γ-treated $Tsc2^{+/-}$ mouse. (d) Summary of pS6 immunohistochemistry analysis showing reduced frequency of pS6-positive kidney cystadenomas in CCI-779-treated (29%, $P < 0.0001$) and IFN-γ-treated (66%, $P = 0.002$) $Tsc2^{+/-}$ mice compared with untreated $Tsc2^{+/-}$ mice (88%). (e) $Tsc2^{-/-}$ tumor staining pS6 positive from an untreated nude mouse. (f) Reduced pS6 staining in a $Tsc2^{-/-}$ tumor from a nude mouse treated with CCI-779. (g) Reduced pS6 staining in a $Tsc2^{-/-}$ tumor from a nude mouse treated with IFN-γ. (h) Reduced pS6 staining in a $Tsc2^{+/+}$ tumor from an untreated nude mouse.

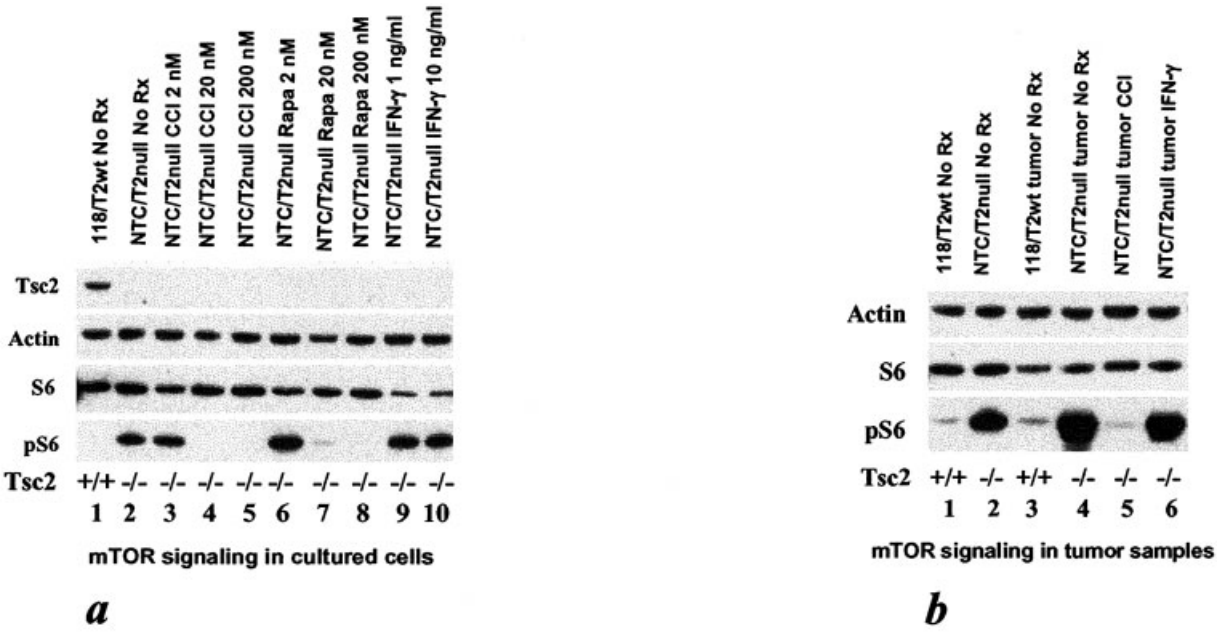

Treatment Group	No Rx	CCI-779	IFN-γ	No Rx
Genotype of tumor cells	Tsc2-/-	Tsc2-/-	Tsc2-/-	Tsc2+/+
		Immunoblot Analysis		
n (mice)	7	4	3	8
Total tumor lysates tested	14	8	8	16
pS6 elevated	14	1	6	0
% pS6 elevated	100%	12.5%	75%	0%
P value (vs. untreated Tsc2-/-)*		<0.0001	0.12	<0.0001
		Immunohistochemistry		
n (mice)	6	4	4	7
Average pS6 grade	2.9 ± 0.1	2.1 ± 0.4	2.6 ± 0.2	1.8 ± 0.2
Range pS6 grade	2.75-3	1-2.75	2-3	1.25-2.25
P value (vs. untreated Tsc2-/-)**		0.03	0.09	<0.0001
*FISHER				
**T TEST				

c

Figure 6. Immunoblot analysis of pS6 levels. (a) Elevated pS6 levels were observed in NTC/T2null cells in culture and were normalized by treatment in vitro (for 4 hr) with either rapamycin or CCI-779 in a dose-dependent manner. NTC/T2null cells were treated with CCI-779, rapamycin, or IFN-γ at the indicated concentrations (lanes 3–10). Untreated controls are shown in lane 1 ($Tsc2^{+/+}$ cells) and lane 2 ($Tsc2^{-/-}$ cells). Total S6, actin, and Tsc2 immunoblot results are also shown. (b) In untreated nude mice, elevated pS6 levels were observed in tumors derived from $Tsc2^{-/-}$ cells (lane 4) but not in tumors from $Tsc2^{+/+}$ cells (lane 3). Decreased pS6 was observed in $Tsc2^{-/-}$ tumors from nude mice treated with CCI-779 (lane 5) as well as with those treated with IFN-γ, but the latter finding was more variable and was not observed in the $Tsc2^{-/-}$ tumor shown in lane 6. Lanes 1 and 2 are control lanes, from the 118/T2wt (lane 1) and NTC/T2null (lane 2) cell lines. Total S6 was similar in all tumor and cell lysate samples; actin is shown as a protein-loading control. (c) Summary of immunoblot (top) and immunohistochemistry (bottom) results from nude mouse tumors.

DISCUSSION

Our finding that both CCI-779 and IFN-γ, when used as single agents, can reduce the severity of kidney cystadenomas in $Tsc2^{+/-}$ mice has direct relevance for the treatment of kidney angiomyolipomas in TSC and LAM patients. We measured the severity of kidney disease by using standard methods (necropsy and quantitative histopathology) as well as MR imaging of the kidneys in these animals. Depending on the method used, there was a 62%–92% reduction in the number of cystadenomas per kidney in $Tsc2^{+/-}$ mice treated with CCI-779 and a 43%–67% reduction in the number of cystadenomas per kidney in $Tsc2^{+/-}$ mice treated with IFN-γ compared with that in an untreated control group. The liver hemangioma results were consistent and may be relevant to the treatment of pulmonary LAM.

The nude mouse model we describe is an important new animal model for TSC because it will permit higher-throughput in vivo screening of drugs that may be effective for the treatment of a variety of TSC lesions. We have demonstrated that treatment with either CCI-779 or IFN-γ reduced tumor growth and prolonged survival in this TSC mouse model. A similar model was used to demonstrate that rapamycin treatment reduced tumor growth in nude mice bearing tumors from a *Tsc2*-deficient cell line derived from a $Tsc2^{+/-}$ mouse kidney tumor (Kobayashi et al., 2003).

Similar to the findings in kidney angiomyolipoma tissue from TSC patients (El-Hashemite et al., 2003b) and other cells/tissues that lack normal hamartin or tuberin (Gao and Pan, 2001; Goncharova et al., 2002; Inoki et al., 2002; Kwiatkowski et al., 2002; Manning et al., 2002; Potter et al., 2002; Zhang et al., 2003a), we observed lack of mTOR inhibition in kidney cystadenomas from untreated $Tsc2^{+/-}$ mice and in tumors that developed in nude mice from $Tsc2^{-/-}$ cells. Both immunohistochemistry and immunoblot analyses demonstrated a dramatic normalization of mTOR signaling with CCI-779 treatment and a modest normalization of mTOR signaling with IFN-γ treatment. Although CCI-779 and rapamycin are direct inhibitors of mTOR kinase, the mechanism by which IFN-γ reduces pS6 levels is not clear. It is likely that the mechanism by which IFN-γ affects mTOR signaling is indirect because the decrease in pS6 in tumors from IFN-γ-treated TSC mouse models was modest and a reduction of pS6 was not observed in cultured $Tsc2^{-/-}$ cells treated with IFN-γ. Although abnormalities in IFN-γ signaling have been observed in tumors and cells lacking the *Tsc1* or *Tsc2* gene (El-Hashemite et al., 2004), the mechanism by which IFN-γ reduces the severity of TSC tumors is the subject of ongoing studies. Potential mechanisms of IFN-γ action include induction of apoptosis (El-Hashemite et al., 2004) and regulation of the cell cycle (Lee and Dabora, unpublished observations).

Although we have emphasized the efficacy of both CCI-779 and IFN-γ as single agents compared with the untreated control group, it is also interesting to compare the CCI-779 treatment group to the IFN-γ treatment group. In $Tsc2^{+/-}$ mice, when disease severity was measured by histopathology analysis or MR imaging, CCI-779 appeared to be more effective than IFN-γ ($P < 0.05$). When severity was measured by necropsy results, no significant difference between the groups was found. Because the duration of CCI-779 treatment was shorter than that of IFN-γ treatment, disease was less severe in the CCI-779 group (by MR imaging and histopathology), and normalization of aberrant mTOR signaling with CCI-779 treatment was dramatic, it appears that CCI-779 (or rapamycin) is the best first-choice agent for testing in clinical trials, but that IFN-γ is an important alternative. It is also important to consider that the combination of CCI-779 and IFN-γ may have synergistic effects with nonoverlapping toxicity profiles. This will be investigated further as well.

TSC is an excellent model disease for demonstrating the utility of developing targeted therapeutic approaches and using genetically engineered mouse models to investigate promising new strategies for treating human diseases. In addition to the significant clinical implications of this work for the treatment of TSC, LAM, and related disorders, we have demonstrated the utility of MR image analysis for evaluating severity of disease in a mouse model of human tumors. This is the first report of MR image analysis in this TSC animal model, and the consistent results between MR imaging findings and standard methods (gross and histopathology) have validated the utility of MR imaging for assessing the severity of kidney disease. Because MR imaging is noninvasive, it will be useful for following kidney disease over time in future preclinical studies.

We have demonstrated that targeted therapy with an mTOR kinase inhibitor, based on the mTOR signaling defect in TSC, dramatically decreased the severity of disease in TSC mouse models. IFN-γ has been identified as a modifier of TSC kidney disease, and a decrease in disease severity

in TSC mouse models treated with exogenous murine IFN-γ also was demonstrated. This finding provides validation for developing treatment strategies based on genetic modifiers. These data provide important preclinical evidence to justify proceeding with well-designed clinical trials to test the efficacy of mTOR kinase inhibitors and IFN-γ in selected patients with TSC and/or LAM. The challenge that remains is to translate these findings safely and efficiently into clinically relevant improvements in the care of patients with TSC, LAM, and related disorders.

ACKNOWLEDGMENTS

We thank Dr. Jay Gibbons, Wyeth Pharmaceuticals, for providing the CCI-779 for this work; Joanne Ingwall, Frank Bunn, Joe Antin, and Tom Stossel for their critical review of the manuscript; Joseph Italiano for the use of his microscope; and Eugenia Shvartz for technical assistance in immunohistochemistry.

REFERENCES

Carsillo T, Astrinidis A, Henske EP. 2000. Mutations in the tuberous sclerosis complex gene TSC2 are a cause of sporadic pulmonary lymphangioleiomyomatosis. Proc Natl Acad Sci USA 97: 6085–6090.

Consortium ECTS. 1993. Identification and characterization of the tuberous sclerosis gene on chromosome 16. Cell 75:1305–1315.

Corradetti MN, Inoki K, Bardeesy N, DePinho RA, Guan KL. 2004. Regulation of the TSC pathway by LKB1: evidence of a molecular link between tuberous sclerosis complex and Peutz-Jeghers syndrome. Genes Dev 18:1533–1538.

Dabora SL, Jozwiak S, Franz DN, Roberts PS, Nieto A, Chung J, Choy YS, Reeve MP, Thiele E, Egelhoff JC, Kasprzyk-Obara J, Domanska-Pakiela D, Kwiatkowski DJ. 2001. Mutational analysis in a cohort of 224 tuberous sclerosis patients indicates increased severity of TSC2, compared with TSC1, disease in multiple organs. Am J Hum Genet 68:64–80.

Dabora SL, Roberts P, Nieto A, Perez R, Jozwiak S, Franz D, Bissler J, Thiele EA, Sims K, Kwiatkowski DJ. 2002. Association between a high-expressing interferon-gamma allele and a lower frequency of kidney angiomyolipomas in TSC2 patients. Am J Hum Genet 71:750–758.

El-Hashemite N, Walker V, Zhang H, Kwiatkowski DJ. 2003a. Loss of Tsc1 or Tsc2 induces vascular endothelial growth factor production through mammalian target of rapamycin. Cancer Res 63:5173–5177.

El-Hashemite N, Zhang H, Henske EP, Kwiatkowski DJ. 2003b. Mutation in TSC2 and activation of mammalian target of rapamycin signalling pathway in renal angiomyolipoma. Lancet 361: 1348–1349.

El-Hashemite N, Zhang H, Walker V, Hoffmeister KM, Kwiatkowski DJ. 2004. Perturbed IFN-gamma-Jak-signal transducers and activators of transcription signaling in tuberous sclerosis mouse models: synergistic effects of rapamycin-IFN-gamma treatment. Cancer Res 64:3436–3443.

Franz DN, Brody A, Meyer C, Leonard J, Chuck G, Dabora S, Sethuraman G, Colby TV, Kwiatkowski DJ, McCormack FX. 2001. Mutational and radiographic analysis of pulmonary disease consistent with lymphangioleiomyomatosis and micronodular pneumocyte hyperplasia in women with tuberous sclerosis. Am J Respir Crit Care Med 164:661–668.

Gao X, Pan D. 2001. TSC1 and TSC2 tumor suppressors antagonize insulin signaling in cell growth. Genes Dev 15:1383–1392.

Garami A, Zwartkruis FJ, Nobukuni T, Joaquin M, Roccio M, Stocker H, Kozma SC, Hafen E, Bos JL, Thomas G. 2003. Insulin activation of Rheb, a mediator of mTOR/S6K/4E-BP signaling, is inhibited by TSC1 and 2. Mol Cell 11:1457–1466.

Gomez M, Sampson J, Whittemore V, editors. 1999. The tuberous sclerosis complex. 3rd ed. Oxford, UK: Oxford University Press.

Goncharova EA, Goncharov DA, Eszterhas A, Hunter DS, Glassberg MK, Yeung RS, Walker CL, Noonan D, Kwiatkowski DJ, Chou MM, Panettieri Jr RA, Krymskaya VP. 2002. Tuberin regulates p70 S6 kinase activation and ribosomal protein S6 phosphorylation. A role for the TSC2 tumor suppressor gene in pulmonary lymphangioleiomyomatosis (LAM). J Biol Chem 277:30958–30967.

Henske EP, Scheithauer BW, Short MP, Wollmann R, Nahmias J, Hornigold N, van Slegtenhorst M, Welsh CT, Kwiatkowski DJ. 1996. Allelic loss is frequent in tuberous sclerosis kidney lesions but rare in brain lesions. Am J Hum Genet 59:400–406.

Henske EP, Wessner LL, Golden J, Scheithauer BW, Vortmeyer AO, Zhuang Z, Klein-Szanto AJ, Kwiatkowski DJ, Yeung RS. 1997. Loss of tuberin in both subependymal giant cell astrocytomas and angiomyolipomas supports a two-hit model for the pathogenesis of tuberous sclerosis tumors. Am J Pathol 151:1639–1647.

Hidalgo M, Rowinsky EK. 2000. The rapamycin-sensitive signal transduction pathway as a target for cancer therapy. Oncogene 19:6680–6686.

Hino O, Kobayashi T, Mitani H. 2002. Prevention of hereditary carcinogenesis. Proc Jpn Acad 78:30–32.

Inoki K, Li Y, Zhu T, Wu J, Guan KL. 2002. TSC2 is phosphorylated and inhibited by Akt and suppresses mTOR signalling. Nat Cell Biol 4:648–657.

Inoki K, Li Y, Xu T, Guan KL. 2003a. Rheb GTPase is a direct target of TSC2 GAP activity and regulates mTOR signaling. Genes & Development 17:1829–1834.

Inoki K, Zhu T, Guan KL. 2003b. TSC2 mediates cellular energy response to control cell growth and survival. Cell 115:577–590.

Jackson SH, Miller GF, Segal BH, Mardiney M, 3rd, Domachowske JB, Gallin JI, Holland SM. 2001. IFN-gamma is effective in reducing infections in the mouse model of chronic granulomatous disease (CGD). J Interferon Cytokine Res 21:567–573.

Kenerson HL, Aicher LD, True LD, Yeung RS. 2002. Activated Mammalian target of rapamycin pathway in the pathogenesis of tuberous sclerosis complex renal tumors. Cancer Res 62:5645–5650.

Kobayashi T, Adachi H, Mitani H, Youko H, Hino O. 2003. Toward chemotherapy for Tsc2-mutant renal tumor. Proc Jpn Acad 79: 22–25.

Kwiatkowski DJ, Zhang H, Bandura JL, Heiberger KM, Glogauer M, el-Hashemite N, Onda H. 2002. A mouse model of TSC1 reveals sex-dependent lethality from liver hemangiomas, and up-regulation of p70S6 kinase activity in Tsc1 null cells. Hum Mol Genet 11:525–534.

Mahalati K, Kahan BD. 2001. Clinical pharmacokinetics of sirolimus. Clin Pharmacokinet 40:573–585.

Manning BD, Tee AR, Logsdon MN, Blenis J, Cantley LC. 2002. Identification of the tuberous sclerosis complex-2 tumor suppressor gene product tuberin as a target of the phosphoinositide 3-kinase/akt pathway. Mol Cell 10:151–162.

National Tuberous Sclerosis Association. 1994. My child has tuberous sclerosis. NTSA educational pamphlet.

Neshat MS, Mellinghoff IK, Tran C, Stiles B, Thomas G, Petersen R, Frost P, Gibbons JJ, Wu H, Sawyers CL. 2001. Enhanced sensitivity of PTEN-deficient tumors to inhibition of FRAP/mTOR. Proc Natl Acad Sci USA 98:10314–10319.

Niida Y, Stemmer-Rachamimov AO, Logrip M, Tapon D, Perez R, Kwiatkowski DJ, Sims K, MacCollin M, Louis DN, Ramesh V. 2001. Survey of somatic mutations in tuberous sclerosis complex (TSC) hamartomas suggests different genetic mechanisms for pathogenesis of TSC lesions. Am J Hum Genet 69:493–503.

Onda H, Lueck A, Marks PW, Warren HB, Kwiatkowski DJ. 1999. TSC2+/− mice develop tumors in multiple sites which express gelsolin and are influenced by genetic background. J Clin Invest 104:687–695.

Online Mendelian Inheritance in Man. 2003a. MIM number 606690. Baltimore, MD: Johns Hopkins University.

Online Mendelian Inheritance in Man. 2003b. MIM numbers 605284 and 191092. Baltimore, MD: Johns Hopkins University.

Podsypanina K, Lee RT, Politis C, Hennessy I, Crane A, Puc J, Neshat M, Wang H, Yang L, Gibbons J, Frost P, Dreisbach V, Blenis J, Gaciong Z, Fisher P, Sawyers C, Hedrick-Ellenson L, Parsons R. 2001. An inhibitor of mTOR reduces neoplasia and normalizes p70/S6 kinase activity in Pten+/− mice. Proc Natl Acad Sci USA 98:10320–10325.

Potter CJ, Huang H, Xu T. 2001. Drosophila Tsc1 functions with

Tsc2 to antagonize insulin signaling in regulating cell growth, cell proliferation, and organ size. Cell 105:357–368.
Potter CJ, Pedraza LG, Xu T. 2002. Akt regulates growth by directly phosphorylating Tsc2. Nat Cell Biol 4:658–665.
Saucedo LJ, Gao X, Chiarelli DA, Li L, Pan D, Edgar BA. 2003. Rheb promotes cell growth as a component of the insulin/TOR signalling network. Nat Cell Biol 5:566–571.
Shi Y, Gera J, Hu L, Hsu JH, Bookstein R, Li W, Lichtenstein A. 2002. Enhanced sensitivity of multiple myeloma cells containing PTEN mutations to CCI-779. Cancer Res 62:5027–5034.
Stocker H, Radimerski T, Schindelholz B, Wittwer F, Belawat P, Daram P, Breuer S, Thomas G, Hafen E. 2003. Rheb is an essential regulator of S6K in controlling cell growth in Drosophila. Nat Cell Biol 5:559–565.
Sullivan EJ. 1998. Lymphangioleiomyomatosis: a review. Chest 114: 1689–1703.
Torrance CJ, Agrawal V, Vogelstein B, Kinzler KW. 2001. Use of isogenic human cancer cells for high-throughput screening and drug discovery. Nat Biotechnol 19:940–945.
van Slegtenhorst M, de Hoogt R, Hermans C, Nellist M, Janssen B, Verhoef S, Lindhout D, van den Ouweland A, Halley D, Young J, Burley M, Jeremiah S, Woodward K, Nahmias J, Fox M, Ekong R, Osborne J, Wolfe J, Povey S, Snell RG, Cheadle JP, Jones AC, Tachataki M, Ravine D, Kwiatkowski DJ. 1997. Identification of the tuberous sclerosis gene TSC1 on chromosome 9q34. Science 277:805–808.
Yu K, Toral-Barza L, Discafani C, Zhang WG, Skotnicki J, Frost P, Gibbons JJ. 2001. mTOR, a novel target in breast cancer: the effect of CCI-779, an mTOR inhibitor, in preclinical models of breast cancer. Endocr Relat Cancer 8:249–258.
Zhang H, Cicchetti G, Onda H, Koon HB, Asrican K, Bajraszewski N, Vazquez F, Carpenter CL, Kwiatkowski DJ. 2003a. Loss of Tsc1/Tsc2 activates mTOR and disrupts PI3K-Akt signalling through downregulation of PDGFR. J Clin Invest 112:1223–1233.
Zhang Y, Gao X, Saucedo LJ, Ru B, Edgar BA, Pan D. 2003b. Rheb is a direct target of the tuberous sclerosis tumour suppressor proteins. Nat Cell Biol 5:578–581.